Steel and Composite Structures, *Vol. 34, No. 5 (2020) 643-655*
DOI: https://doi.org/10.12989/scs.2020.34.5.643

Buckling behavior of a single-layered graphene sheet resting on viscoelastic medium via nonlocal four-unknown integral model

Moussa Bellal[1], Habib Hebali[2,3], Houari Heireche[1], Abdelmoumen Anis Bousahla[1,4], Abdeldjebbar Tounsi [1,4], Fouad Bourada[2,5], S.R. Mahmoud[6], E.A. Adda Bedia[4] and Abdelouahed Tounsi [*2,4]

[1]*Laboratoire de Modélisation et Simulation Multi-échelle, Département de Physique, Faculté des Sciences Exactes, Département de Physique, Université de Sidi Bel Abbés, Algeria*
[2]*Material and Hydrology Laboratory, University of Sidi Bel Abbes, Faculty of Technology, Civil Engineering Department, Algeria*
[3]*University Mustapha Stambouli of Mascara, Civil Engineering Department, Mascara, Algeria*
[4]*Department of Civil and Environmental Engineering, King Fahd University of Petroleum & Minerals, 31261 Dhahran, Eastern Province, Saudi Arabia*
[5]*Département des Sciences et de la Technologie, centre universitaire de Tissemsilt, BP 38004 Ben Hamouda, Algeria*
[6]*GRC Department, Jeddah Community College, King Abdulaziz University, Jeddah, Saudi Arabia*

(*Received November 10, 2019, Revised January 23, 2020, Accepted February 6, 20120*)

Abstract. In the present work, the buckling behavior of a single-layered graphene sheet (SLGS) embedded in visco-Pasternak's medium is studied using nonlocal four-unknown integral model. This model has a displacement field with integral terms which includes the effect of transverse shear deformation without using shear correction factors. The visco-Pasternak's medium is introduced by considering the damping effect to the classical foundation model which modeled by the linear Winkler's coefficient and Pasternak's (shear) foundation coefficient. The SLGS under consideration is subjected to compressive in- plane edge loads per unit length. The influences of many parameters such as nonlocal parameter, geometric ratio, the visco-Pasternak's coefficients, damping parameter, and mode numbers on the buckling response of the SLGSs are studied and discussed.

Keywords: non-uniform buckling; four-unknown integral model; nonlocal elasticity theory; visco-Pasternak's medium

1. Introduction

Since the discovery of graphene by Novoselov et al. (2004), numerous investigations have been published in the literature on the vibration, buckling and wave propagation of graphene sheets. Graphene is a monolayer disposed in a honeycomb network with a unique series of "unprecedented structural", mechanical and electrical characteristics (Basua and Bhattacharyya 2012). Nanostructural elements include nano-tubes, nano-beams, nano-plates, nano-sheets and nano-cones. Nanostructure components have many applications in micro/nano electromechanical systems (MEMS / NEMS), nano sensors, electric batteries, biomedical,bioelectric, compositereinforcement, etc. (Lim *et al.* 2010, Ghorbanpour Arani *et al.* 2014, Sakhaee-Pour *et al.* 2008, Wang *et al.* 2012, Li *et al.* 2011, Pantelic *et al*. 2012, Eltaher *et al.* 2013, Eltaher *et al.* 2016, Ebrahimi and Barati 2017a,b, Akbaş 2016, 2018, Eltaher *et al*. 2018, Hamidi *et al.* 2018, Belmahi *et al.* 2018, Dihaj *et al*. 2018, Bensattalah *et al*. 2018ab, Mohamed *et al.* 2019, Eltaher *et al.* 2019, Belmahi *et al.* 2019, Bensattalah *et al*. 2019, Barati *et al*. 2019 , Forsat *et al*. 2020). Because of their potential, graphene sheets are used in nanotechnology, particularly in recent years.

In order to investigate the mechanical response of nanoscale structures, it has been shown that the small-scale impact should play a considerable role in nanostructures, but this small-scale impact was ignored when adopting the classical local continuum theory (Xu *et al*. 2013). Recently, different size-dependent continuum models such as "couple stress theory" (Reddy 2011), "strain gradient elasticity theory" (Akgöz and Civalek 2013a, b, Lam *et al.* 2003, Karami and Janghorban 2019, Karami and Karami 2019), "modified couple stress theory" (Ke *et al.* 2012, Akgöz and Civalek 2011, Akgöz and Civalek 2013c, Yang *et al*. 2002, Akgöz and Civalek 2012) and "nonlocal elasticity theory" (Eringen and Edelen 1972, Eringen 1983, 2002, 2006) are developed. These theories include information on interatomic forces and internal lengths introduced as a small-scale effect in non-local elasticity theory (Eringen 2006).

In this regard, Pradhan and Murmu (2009) investigated the small-scale influence on stability analysis of biaxially-compressed single-layered graphene sheets (SLGSs) employing non-local continuum mechanics. Sakhaee-Pour (2008) studied the elastic buckling response of flawless SLGS using an atomistic modeling formulation. Farajpour *et al.* (2013a) studied the nonlinear buckling properties of

*Corresponding author, Professor
E-mail: tou_abdel@yahoo.com

ISSN: 1229-9367 (Print), 1598-6233 (Online)

MLGS under non-uniformly varied in-plane load across the thickness. Farajpour *et al.* (2013b) studied the axisymmetric stability analysis of circular SLGS by uncoupling basic constitutive equations based on the Eringen non-local theory. Ansari and Sahmani (2013) studied the biaxial stability response of SLGS. They introduced Eringen's non-local elasticity equations into different plate models to account for the size effects in the analysis. Mohammadi *et al.* (2014) studied the stability response of an orthotropic rectangular nanoscale plate. They implemented the non-local elasticity theory to study the shear buckling of orthotropic SLGS in a "thermal environment".

The literature shows that research on integrated SLGS or MLGS in an elastic medium is becoming more common for more accurate design and investigation of micro and nanostructures. Pradhan and Murmu (2010) studied the SLGS buckling behavior integrated in an elastic medium by implementing the theory of nonlocal elasticity based on "classical plate theory". Samaei *et al.* (2011) examined the effect of the length scale on the buckling response of an integrated SLGS in a Pasternak elastic medium using non-local Mindlin plate theory. Radic *et al.* (2014) presented the buckling of double orthotropic nanoplates based on the theory of nonlocal elasticity. They assumed that two nanoplates are bound by an internal elastic medium and surrounded by an external elastic base. Anjomshoa *et al.* (2014) developed a finite element formulation based on non-local elasticity theory for buckling analysis of nanoscale MLGS incorporated into a polymer matrix. Golmakani and Rezatalab (2015) studied the non-uniform biaxial buckling analysis of integrated orthotropic SLGS in an elastic medium of Pasternak using the nonlocal Mindlin plate model to derive equilibrium equations for nanoplates in terms of generalized displacements. Karlicic *et al.* (2015) presented the analysis of the thermal stability and vibration of multilayered graphene sheets modeled as a multi-nanoplates system integrated in an elastic medium using the non-local plate theory of Kirchhoff-Love to deduce the basic equations and determine their exact analytical solutions for non-local frequencies, "critical buckling loads", and "critical buckling temperature" using Navier method. Zhang *et al*. (2016) discussed the "critical buckling loads" of SLGSs by using the "element free kp-Ritz method". Zenkour (2016) investigated the buckling response of a SLGS embedded in visco-Pasternak's medium using nonlocal first-order theory. Liu *et al.* (2016) studied bending, buckling and vibration of graphenenanosheets using on the nonlocal theory. Recently, Safaei *et al.* (2019) presented a non-classical plate model for SLGS for axial buckling. Based on nonlocal elasticity theory, Soleimani *et al.* (2019) examined the effect of out-of-plane defects on the postbuckling behavior of graphene sheets.

Despite extensive research on buckling behaviors of SLGSs utilizing non-local elasticity theory, there are few studies taking into account non-local visco-elastic systems. However, to our knowledge, no work has been found in the literature on the non-uniform buckling analyzes of graphene sheets incorporated into a viscoelastic medium via non-local high shear deformation theory. Motivated by these findings, in order to improve the design of the coupled nano system, our objective is to investigate the buckling analysis of the visco SLGSs system based on the higher order shear deformation theory. This model has a displacement field with integral terms which includes the effect of transverse shear deformation without using shear correction factors SLGS carry viscous fluids and are coupled by visco-Pasternak's medium. The analytical solutions are determined to demonstrate the characteristic parameters of coupled visco-SLGSs. The results of this work should be used to design this type of nano-devices.

2. Theoretical formulation

In this work, a SLGS of length a, width b and uniform thickness h is considered as shown in Fig. 1. The SLGS is supposed to be subjected to distributive compressive in-plane edge loads S_1 and S_2 per unit length. The foundation model is characterized by the linear Winkler's modulus K_w, the Pasternak's (shear) foundation modulus K_p, and the damping coefficient C_t of the viscoelastic medium.

2.1 The four-unknown integral model

The four-unknown integral model is employed for the examined SLGS. The displacement field is expressed as

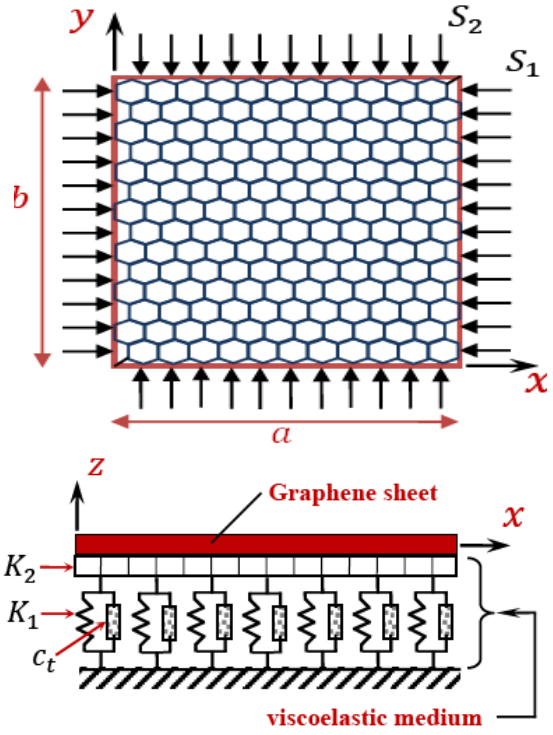

Fig. 1 Continuum plate model of a SLGS sheet embedded in a viscoelastic medium

$$\begin{aligned} u(x,y,z) &= u_0(x,y) - z\frac{\partial w(x,y,z)}{\partial x} + f(z)k_1\int\theta(x,y)dx \\ v(x,y,z) &= v_0(x,y) - z\frac{\partial w(x,y,z)}{\partial y} + f(z)k_2\int\theta(x,y)dy \\ w(x,y,z) &= w_0(x,y) \end{aligned} \tag{1}$$

It can be observed that the displacement field in Eq. (1) introduces only four unknowns (u_0, v_0, w_0 and θ). In this work, the present higher-order shear deformation plate theory is obtained by setting

$$f(z) = \frac{h}{\pi}\sin\left(\frac{\pi z}{h}\right) \tag{2}$$

The nonzero strains associated with the displacement field in Eq. (1) are

$$\begin{Bmatrix}\varepsilon_x\\ \varepsilon_y\\ \gamma_{xy}\end{Bmatrix} = \begin{Bmatrix}\varepsilon_x^0\\ \varepsilon_y^0\\ \gamma_{xy}^0\end{Bmatrix} + z\begin{Bmatrix}k_x^b\\ k_y^b\\ k_{xy}^b\end{Bmatrix} + f(z)\begin{Bmatrix}k_x^s\\ k_y^s\\ k_{xy}^s\end{Bmatrix}, \qquad \begin{Bmatrix}\gamma_{yz}\\ \gamma_{xz}\end{Bmatrix} = g(z)\begin{Bmatrix}\gamma_{yz}^0\\ \gamma_{xz}^0\end{Bmatrix}, \tag{3}$$

Where

$$\begin{Bmatrix}\varepsilon_x^0\\ \varepsilon_y^0\\ \gamma_{xy}^0\end{Bmatrix} = \begin{Bmatrix}\dfrac{\partial u_0}{\partial x}\\ \dfrac{\partial v_0}{\partial x}\\ \dfrac{\partial u_0}{\partial y} + \dfrac{\partial v_0}{\partial x}\end{Bmatrix}, \begin{Bmatrix}k_x^b\\ k_y^b\\ k_{xy}^b\end{Bmatrix} = \begin{Bmatrix}-\dfrac{\partial^2 w_0}{\partial x^2}\\ -\dfrac{\partial^2 w_0}{\partial y^2}\\ -2\dfrac{\partial^2 w_0}{\partial x\partial y}\end{Bmatrix}, \tag{4a}$$

$$\begin{Bmatrix}k_x^s\\ k_y^s\\ k_{xy}^s\end{Bmatrix} = \begin{Bmatrix}k_1\theta\\ k_2\theta\\ k_1\dfrac{\partial}{\partial y}\int\theta\,dx + k_2\dfrac{\partial}{\partial x}\int\theta\,dy\end{Bmatrix}, \quad \begin{Bmatrix}\gamma_{yz}^0\\ \gamma_{xz}^0\end{Bmatrix} = \begin{Bmatrix}k_2\int\theta\,dy\\ k_1\int\theta\,dx\end{Bmatrix},$$

And

$$g(z) = \frac{df(z)}{dz} \tag{4b}$$

The integrals defined in the above equations shall be resolved by a Navier type method and can be written as follows

$$\frac{\partial}{\partial y}\int\theta\,dx = A'\frac{\partial^2\theta}{\partial x\partial y}, \quad \frac{\partial}{\partial x}\int\theta\,dy = B'\frac{\partial^2\theta}{\partial x\partial y}, \quad \int\theta\,dx = A'\frac{\partial\theta}{\partial x}, \quad \int\theta\,dy = B'\frac{\partial\theta}{\partial y} \tag{5}$$

Where the coefficients A' and B' are expressed according to the type of solution used, in this case via Navier. Therefore, A', B', k_1 and k_2 are expressed as follows

$$A' = -\frac{1}{\lambda^2}, \quad B' = -\frac{1}{\mu^2}, k_1 = \lambda^2, k_2 = \mu^2 \tag{6}$$

Where λ and μ are defined in expression (20).

The governing equations of SLGS resting on visco-Pasternak's medium under distributive compressive in-plane edge loads may be deduced on the basis of the "stationary potential energy" (Reddy 1984). The governing equations are determined as

$$\begin{aligned} &\frac{\partial N_x}{\partial x} + \frac{\partial N_{xy}}{\partial y} = 0 \\ &\frac{\partial N_{xy}}{\partial x} + \frac{\partial N_y}{\partial y} = 0 \\ &\frac{\partial^2 M_x^b}{\partial x^2} + \frac{\partial^2 M_y^b}{\partial y^2} + 2\frac{\partial^2 M_{xy}^b}{\partial x\partial y} - P(x,y) = 0 \\ &k_1 A'\frac{\partial^2 M_x^s}{\partial x^2} + k_2 B'\frac{\partial^2 M_y^s}{\partial y^2} + \left(k_1 A' + k_2 B'\right)\frac{\partial^2 M_{xy}^s}{\partial x\partial y} - k_1 A'\frac{\partial Q_x}{\partial x} - k_2 B'\frac{\partial Q_y}{\partial y} = 0 \end{aligned} \tag{7}$$

where

$$\begin{aligned} P(x,y) = K_w w - K_p\left(\frac{\partial^2 w}{\partial x^2} + \frac{\partial^2 w}{\partial y^2}\right) + C_t\frac{\partial w}{\partial t} \\ -\frac{\partial}{\partial x}\left(S_1\frac{\partial w}{\partial x}\right) - \frac{\partial}{\partial y}\left(S_2\frac{\partial w}{\partial y}\right) \end{aligned} \tag{8}$$

andstress resultants N, M, and Q are defined by

$$\begin{Bmatrix} N_x & N_y & N_{xy} \\ M_x^b & M_y^b & M_{xy}^b \\ M_x^s & M_y^s & M_{xy}^s \end{Bmatrix} = \int_{-h/2}^{h/2}\begin{Bmatrix}1\\ z\\ f(z)\end{Bmatrix}dz \tag{9a}$$

$$\left(Q_x, Q_y\right) = \int_{-h/2}^{h/2}\left(\tau_{xz}, \tau_{yz}\right)g(z)dz \tag{9b}$$

2.2 The nonlocal elasticity model for SLGS

Based on Eringen's nonlocal elasticity theory (Eringen 1972), the stress state at a point inside a body is considered to be a function of strains of all points in the neighbor regions. For homogeneous elastic solids, the nonlocal stress-tensor components σ_{ij} at each point x in the solid can be expressed as

$$\sigma_{ij}(x) = \int_{\Omega}\alpha\left(|x'-x|, \tau\right)t_{ij}(x')d\Omega(x') \tag{10}$$

where $t_{ij}(x')$ are the components available in local stress tensor at point x which are related to the strain tensor components ε_{kl} as

$$t_{ij} = C_{ijkl}\varepsilon_{kl} \tag{11}$$

The concept of Eq. (10) is that the nonlocal stress at any point is a weighting average of the local stress of all near

points, and the nonlocal kernel $\alpha\left(|x'-x|,\ \tau\right)$ considers the effect of the strain at the point x' on the stress at the point x in the elastic body. The parameter α is an internal characteristic length (e.g., lattice parameter, granular distance, the length of C–C bonds). Also $|x'-x|$ is Euclidean distance and τ is a constant value as follows

$$\tau = \frac{e_0 a}{l} \tag{12}$$

which defines the relation of a characteristic internal length, and a characteristic external length, l (e.g., crack length and wavelength) by employing a constant, e_0 ,dependent on each material. Eringen (1972, 1983) numerically obtain the functional form of the kernel. By appropriate selection of the kernel function, Eringen shown that the nonlocal constitutive equation given in integral form (see Eq. (13)) can be represented in an equivalent differential form as

$$\left(1-(e_0 a)\nabla^2\right)\sigma_{kl} = t_{kl} \tag{13}$$

In which ∇^2 is the Laplacian operator. Hence, the scale length $e_0 a$ considers the effects of small size on the behavior of nanostructures. Thus, the constitutive relations of nonlocal theory for a SLGS can be written as

$$\left(1-\zeta\nabla^2\right)\begin{Bmatrix}\sigma_x\\ \sigma_y\\ \tau_{xy}\\ \tau_{yz}\\ \tau_{xz}\end{Bmatrix} = \begin{bmatrix}C_{11} & C_{12} & 0 & 0 & 0\\ C_{12} & C_{22} & 0 & 0 & 0\\ 0 & 0 & C_{66} & 0 & 0\\ 0 & 0 & 0 & C_{55} & 0\\ 0 & 0 & 0 & 0 & C_{44}\end{bmatrix}\begin{Bmatrix}\varepsilon_x\\ \varepsilon_y\\ \gamma_{xy}\\ \gamma_{yz}\\ \gamma_{xz}\end{Bmatrix} \tag{14}$$

In which $\zeta = (e_0 a)^2$ and the stiffness coefficients, C_{ij} , can be defined as

$$C_{11} = C_{22} = \frac{E}{1-\nu^2},\ C_{12} = \frac{\nu E}{1-\nu^2},\qquad C_{44} = C_{55} = C_{66} = \frac{E}{2[1+\nu]}, \tag{15}$$

Integrating Eq. (14) over the plate's cross-section area yields the force–strain and the moment–strain of the nonlocal refined SLGS as follows

$$\left(1-\zeta\nabla^2\right)\begin{Bmatrix}N_x\\ N_y\\ N_{xy}\\ M_x^b\\ M_y^b\\ M_{xy}^b\\ M_x^s\\ M_y^s\\ M_{xy}^s\end{Bmatrix} = \begin{bmatrix}A_{11} & A_{12} & 0 & B_{11} & B_{12} & 0 & B_{11}^s & B_{12}^s & 0\\ A_{12} & A_{22} & 0 & B_{12} & B_{22} & 0 & B_{12}^s & B_{22}^s & 0\\ 0 & 0 & A_{66} & 0 & 0 & B_{66} & 0 & 0 & B_{66}^s\\ B_{11} & B_{12} & 0 & D_{11} & D_{12} & 0 & D_{11}^s & D_{12}^s & 0\\ B_{12} & B_{22} & 0 & D_{12} & D_{22} & 0 & D_{12}^s & D_{22}^s & 0\\ 0 & 0 & B_{66} & 0 & 0 & D_{66} & 0 & 0 & D_{66}^s\\ B_{11}^s & B_{12}^s & 0 & D_{11}^s & D_{12}^s & 0 & H_{11}^s & H_{12}^s & 0\\ B_{12}^s & B_{22}^s & 0 & D_{12}^s & D_{22}^s & 0 & H_{12}^s & H_{22}^s & 0\\ 0 & 0 & B_{66}^s & 0 & 0 & D_{66}^s & 0 & 0 & H_{66}^s\end{bmatrix}\begin{Bmatrix}\varepsilon_x^0\\ \varepsilon_y^0\\ \gamma_{xy}^0\\ k_x^b\\ k_y^b\\ k_{xy}^b\\ k_x^s\\ k_y^s\\ k_{xy}^s\end{Bmatrix} \tag{16a}$$

$$\left(1-\zeta\nabla^2\right)\begin{Bmatrix}S_{xz}^s\\ S_{yz}^s\end{Bmatrix} = \begin{bmatrix}A_{55}^s & 0\\ 0 & A_{44}^s\end{bmatrix}\begin{Bmatrix}\gamma_{xz}^0\\ \gamma_{yz}^0\end{Bmatrix} \tag{16b}$$

Where the cross-sectional rigidities are defined as follows

$$\left(A_{ij}, B_{ij}, D_{ij}, B_{ij}^s, D_{ij}^s, H_{ij}^s\right) = \int_{-h/2}^{h/2} C_{ij}\left(1, z, z^2, f(z), z\,f(z), f^2(z)\right)dz,\quad (i,j=1,2,6) \tag{17a}$$

$$A_{ij}^s = \int_{-h/2}^{h/2} C_{ij}\left[g(z)\right]^2 dz,\quad (i,j=4,5) \tag{17b}$$

The nonlocal equations of stability of SLGS in terms of the displacement can be obtained by substituting Eqs. (16), into Eqs. (7) as follows

$$\begin{aligned}&A_{11}\frac{\partial^2 u_0}{\partial x^2} + A_{66}\frac{\partial^2 u_0}{\partial y^2} + \left(A_{12}+A_{66}\right)\frac{\partial^2 v_0}{\partial x\,\partial y} - B_{11}\frac{\partial^3 w_0}{\partial x^3} - \left(B_{12}+2B_{66}\right)\frac{\partial^3 w_0}{\partial x\,\partial y^2}\\ &+\left(B_{66}^s\left(k_1 A'+k_2 B'\right)\right)\frac{\partial^3\theta}{\partial x\,\partial y^2} + \left(B_{11}^s k_1 + B_{12}^s k_2\right)\frac{\partial\theta}{\partial x} = 0\end{aligned} \tag{18a}$$

$$\begin{aligned}&A_{22}\frac{\partial^2 v_0}{\partial y^2} + A_{66}\frac{\partial^2 v_0}{\partial x^2} + \left(A_{12}+A_{66}\right)\frac{\partial^2 u_0}{\partial x\,\partial y} - B_{22}\frac{\partial^3 w_0}{\partial y^3}\\ &-\left(B_{12}+2B_{66}\right)\frac{\partial^3 w_0}{\partial x^2\partial y} + \left(B_{66}^s\left(k_1 A'+k_2 B'\right)\right)\frac{\partial^3\theta}{\partial x^2\partial y}\\ &+\left(B_{22}^s k_2 + B_{12}^s k_1\right)\frac{\partial\theta}{\partial y} = 0\end{aligned} \tag{18b}$$

$$\begin{aligned}&B_{11}\frac{\partial^3 u_0}{\partial x^3} + \left(B_{12}+2B_{66}\right)\frac{\partial^3 u_0}{\partial x\,\partial y^2} + \left(B_{12}+2B_{66}\right)\frac{\partial^3 v_0}{\partial x^2\,\partial y} +\\ &B_{22}\frac{\partial^3 v_0}{\partial y^3} - D_{11}\frac{\partial^4 w_0}{\partial x^4} - 2\left(D_{12}+2D_{66}\right)\frac{\partial^4 w_0}{\partial x^2\partial y^2} - D_{22}\frac{\partial^4 w_0}{\partial y^4}\\ &+\left(D_{11}^s k_1 + D_{12}^s k_2\right)\frac{\partial^2\theta}{\partial x^2} + 2\left(D_{66}^s\left(k_1 A'+k_2 B'\right)\right)\frac{\partial^4\theta}{\partial x^2\partial y^2} +\\ &\left(D_{12}^s k_1 + D_{22}^s k_2\right)\frac{\partial^2\theta}{\partial y^2} + \left(1-\mu\nabla^2\right)P(x,y) = 0\end{aligned} \tag{18c}$$

$$\begin{aligned}&-\left(B_{11}^s k_1 + B_{12}^s k_2\right)\frac{\partial u_0}{\partial x} - \left(B_{66}^s\left(k_1 A'+k_2 B'\right)\right)\frac{\partial^3 u_0}{\partial x\partial y^2}\\ &-\left(B_{66}^s\left(k_1 A'+k_2 B'\right)\right)\frac{\partial^3 v_0}{\partial x^2\partial y} - \left(B_{12}^s k_1 + B_{22}^s k_2\right)\frac{\partial v_0}{\partial y}\\ &+\left(D_{11}^s k_1 + D_{12}^s k_2\right)\frac{\partial^2 w_0}{\partial x^2} + 2\left(D_{66}^s\left(k_1 A'+k_2 B'\right)\right)\frac{\partial^4 w_0}{\partial x^2\partial y^2}\\ &+\left(D_{12}^s k_1 + D_{22}^s k_2\right)\frac{\partial^2 w_0}{\partial y^2} - H_{11}^s k_1^2\,\theta - H_{22}^s\,k_2^2\,\theta\\ &-2H_{12}^s k_1 k_2\theta - \left(\left(k_1 A'+k_2 B'\right)^2 H_{66}^s\right)\frac{\partial^4\theta}{\partial x^2\partial y^2}\\ &+A_{44}^s\left(k_2 B'\right)^2\frac{\partial^2\theta}{\partial y^2} + A_{55}^s\left(k_1 A'\right)^2\frac{\partial^2\theta}{\partial x^2} = 0\end{aligned} \tag{18d}$$

3. Solution procedures

In this section, an analytical solution based on the

Navier method is employed to solve the nonlocal governing equations of a simply supported SLGS. The displacement variables are adopted to be of the form

$$\begin{Bmatrix} u_0 \\ v_0 \\ w_0 \\ \theta \end{Bmatrix} = \sum_{m=1}^{\infty}\sum_{n=1}^{\infty} \begin{Bmatrix} U_{mn}\cos(\lambda x)\sin(\mu y) \\ V_{mn}\sin(\lambda x)\cos(\mu y) \\ W_{mn}\sin(\lambda x)\sin(\mu y) \\ X_{mn}\sin(\lambda x)\sin(\mu y) \end{Bmatrix} e^{\omega t} \tag{19}$$

where (U_{mn}, V_{mn}, W_{mn}, X_{mn}) are the unknown Fourier coefficients.with

$$\lambda = m\pi / a \quad \text{and} \quad \mu = n\pi / b \tag{20}$$

Inserting Eq. (19) into Eqs. (18), leads to

$$\begin{bmatrix} S_{11} & S_{12} & S_{13} & S_{14} \\ S_{12} & S_{22} & S_{23} & S_{24} \\ S_{13} & S_{23} & S_{33}+P^* & S_{34} \\ S_{14} & S_{24} & S_{34} & S_{44} \end{bmatrix} \begin{Bmatrix} U_{mn} \\ V_{mn} \\ W_{mn} \\ X_{mn} \end{Bmatrix} = \begin{Bmatrix} 0 \\ 0 \\ 0 \\ 0 \end{Bmatrix} \tag{21}$$

where

$$\begin{aligned}
&S_{11} = -\left(A_{11}\lambda^2 + A_{66}\mu^2\right), \\
&S_{12} = -\lambda\mu\left(A_{12} + A_{66}\right), \\
&S_{13} = \lambda\left(B_{11}\lambda^2 + B_{12}\mu^2 + 2B_{66}\mu^2\right), \\
&S_{14} = \lambda\left(k_1 B^s_{11} + k_2 B^s_{12} - \left(k_1 A' + k_2 B'\right)B^s_{66}\mu^2\right), \\
&S_{22} = -\left(A_{66}\lambda^2 + A_{22}\mu^2\right), \\
&S_{23} = \mu\left(B_{22}\mu^2 + B_{12}\lambda^2 + 2B_{66}\lambda^2\right), \\
&S_{24} = \mu\left(k_2 B^s_{22} + k_1 B^s_{12} - \left(k_1 A' + k_2 B'\right)B^s_{66}\lambda^2\right) \\
&S_{33} = -\left(D_{11}\alpha^4 + 2(D_{12} + 2D_{66})\alpha^2\beta^2 + D_{22}\beta^4\right) \\
&+\lambda\left(k_w + \left(N^T + k_s\right)\left(\alpha^2 + \beta^2\right)\right), \\
&S_{34} = -k_1\left(D^s_{11}\alpha^2 + D^s_{12}\beta^2\right) + 2(k_1 A' + k_2 B')\,D^s_{66}\alpha^2\beta^2 \\
&-k_2\left(D^s_{22}\beta^2 + D^s_{12}\alpha^2\right), \\
&S_{44} = -k_1\left(H^s_{11}k_1 + H^s_{12}k_2\right) - (k_1 A' + k_2 B')^2 H^s_{66}\alpha^2\beta^2 \\
&-k_2\left(H^s_{12}k_1 + H^s_{22}k_2\right) - \left(k_1 A'\right)^2 A^s_{55}\alpha^2 - \left(k_2 B'\right)^2 A^s_{44}\beta^2 \\
&\lambda = 1 + \mu\left(\alpha^2 + \beta^2\right) \\
&P^* = -\left[1 + \zeta\left(\lambda^2 + \mu^2\right)\right]\times \\
&\left(k_w + k_p\left(\lambda^2 + \mu^2\right) + C_t\ \omega + S_1\lambda^2 - S_2\mu^2\right)W_{mn}
\end{aligned} \tag{22}$$

Assuming that there is a given ratio between these forces such that $S_1 = -\beta_0$ and $S_2 = -\alpha\,\beta_0$; $\alpha = S_2 / S_1$ (here α is non-dimensional load parameter)

Thus, we get the buckling equation by setting the $\det[K] = 0$. Solving this equation, we shall find that the assumed buckling of the SLGS is possible only for definite values of β_0. The smallest of these values determines the desired critical value.

In the case where the forces S_1 and S_2 are not constants, the problem becomes more involved, since Eq. (21) has in this case variable coefficients, but the general conclusion remains the same. Let, for example (Timoshenko and Gere 1961)

$$S_1 = -\beta_0\left(1 - c\frac{y}{b}\right), \quad S_2 = 0 \tag{23}$$

where c is a buckling factor. If $c = 0$ the compressive force is uniformly distributed ($S_1 = -\beta_0$, $S_2 = 0$) and if $c = 2$ we obtain the case of pure bending. All other values give a combination of bending and compression ($c < 2$) or tension ($c > 2$).

4. Numerical results and discussions

In this work, the "buckling loads" for the considered SLGSs are calculated with and without the consideration of scale coefficient ζ. The following non-dimensional quantities are used

$$\beta = \frac{a^2}{D}\beta_0, \quad k_w = \frac{a^2}{D}K_w, \quad k_p = \frac{a^2}{D}K_p, \quad \overline{C}_t = \frac{a^4 C_t}{10^3 D}, \quad \eta = \sqrt{\frac{\zeta}{a}} \tag{24}$$

It should be noted that, we get the "buckling equation" of the SLGSs by employing the theory of local elasticity by taking $\zeta = 0$ in Eq. (16).

In the first part, the calculated results are compared to those of the buckling analysis of the SLGSs just embedded in an elastic medium (Samaei *et al*. 2011, Golmakani and Rezatalab 2015), without any elastic foundations (Pradhan and Murmu 2009, Ansari and Sahmani 2013, Hosseini-Hashemi *et al*. 2015) or embedded in a viscoelastic medium (Zenkour 2016).

In the first example, mechanical properties of SLGS are taken as E = 1 TPa and ν = 0.16. Also, the thickness and the scale influence are taken as h = 0.34 nm and ζ = 1.81 nm2. The calculated results for the uniform nonlocal biaxial "buckling load" β_0 (nN) of an isotropic square SLGS are compared with those of molecular dynamic (MD) as provided by Ansari and Sahmani (2013), of differential quadrature method (DQM) reported by Golmakani and Rezatalab (2015) and of the FSDT given by Zenkour (2016) in Table 1. It can be observed that there is a very good agreement with the results of other similar works. The present model does not use the shear correction factor as is considered by Zenkour (2016). It should be indicated that the current model use only four variables, which is even less than the FSDT of Zenkour (2016). As presented in Table 1, it is clear that β_0 is reduced with increasing the "dimension of the SLGS".

Table 1 Comparison of critical biaxial buckling load β_0 of nonlocal square SLGSs with those of MD (Ansari and Sahmani 2013) and of DQM (Golmakani and Rezatalab 2015)

a (nm)	MD (Ansari and Sahmani 2013)	DQM (Golmakani and Rezatalab 2015)	β_0			
			Zenkour (2016) FSDT	Present CPT	Present FSDT	Present HSDT
4.990	1.0837	1.0749	1.07103	1.09440	1.07103	1.07107
8.080	0.6536	0.6523	0.65143	0.65685	0.65143	0.65144
10.77	0.4331	0.4356	0.43529	0.43732	0.43528	0.43529
14.65	0.2609	0.2645	0.26436	0.26503	0.26436	0.26436
18.51	0.1714	0.1751	0.17509	0.17537	0.17509	0.17509
22.35	0.1191	0.1239	0.12383	0.12396	0.12383	0.12383
26.22	0.0889	0.0917	0.09167	0.09174	0.09167	0.09167
30.04	0.0691	0.0707	0.07068	0.07073	0.07068	0.07068
33.85	0.0554	0.0561	0.05613	0.05616	0.05613	0.05613
37.81	0.0449	0.0453	0.04526	0.04528	0.04526	0.04526
41.78	0.0372	0.0372	0.03724	0.03725	0.03724	0.03724
45.66	0.0315	0.0313	0.03128	0.03129	0.03128	0.03128

Table 2 Comparison of dimensionless critical buckling load β and critical buckling load ratio of nonlocal square SLGSs ($h/a=0.1$)

	$\sqrt{\zeta}$	β				β_{NL}/β_L					
		Present CPT	Present FSDT	Present HSDT	Zenkour (2016)	Present CPT	Present FSDT	Present HSDT	Zenkour (2016)	Pradhan and Murmu (2009)	Hosseini-Hashemi*et al.* (2015)
5	0.5	16.4852	15.6051	15.6070	15.6051	0.8351	0.8351	0.8351	0.8352	0.8350	0.8350
	1.0	11.0302	10.4413	10.4426	10.4413	0.5588	0.5588	0.5588	0.5588	0.6500	0.5590
	1.5	7.1093	6.7298	6.7306	6.7298	0.3602	0.3602	0.3602	0.3602	0.3610	0.3600
	2.0	4.7470	4.4935	4.4941	4.4935	0.2405	0.2405	0.2405	0.2405	0.2420	0.2410
10	0.5	18.8109	17.8067	17.8088	17.8067	0.9530	0.9530	0.9530	0.9530	0.9540	0.9530
	1.0	16.4852	15.6051	15.6070	15.6051	0.8351	0.8351	0.8351	0.8351	0.8360	0.8350
	1.5	13.6686	12.9388	12.9404	12.9388	0.6925	0.6925	0.6925	0.6925	0.6930	0.6920
	2.0	11.0302	10.4413	10.4426	10.4413	0.5588	0.5588	0.5588	0.5588	0.5600	0.5590
25	0.5	19.5846	18.5390	18.5413	18.5390	0.9922	0.9922	0.9922	0.9922	0.9930	0.9920
	1.0	19.1349	18.1133	18.1155	18.1133	0.9694	0.9694	0.9694	0.9694	0.9700	0.9690
	1.5	18.4296	17.4457	17.4478	17.4457	0.9337	0.9337	0.9337	0.9337	0.9350	0.9310
	2.0	17.5252	16.5896	16.5916	16.5896	0.8878	0.8878	0.8878	0.8878	0.8890	0.8880

We define in this study the "buckling load ratio" as β_{NL}/β_L where β_{NL} is the "buckling load" obtained by employing the nonlocal theory and β_L is the "buckling load" obtained by employing the local theory. In Tables 1 and 2, we are taking $\overline{C}_t = k_w = k_p = 0$. The values of "Young's modulus" $E = 30\,10^6\,\text{Pa}$ and "Poisson's ratio" $\nu = 0.3$ are considered to compute the numerical values.

Table 2 presents a comparison on the "critical buckling load" ratios determined by the present analytical solution (α =1) and the solutions of Pradhan and Murmu (2009), Zenkour (2016) and Hosseini-Hashemi *et al.* (2015) for a square SLGS with various side lengths and scale parameters. A very good agreement can be shown between the calculated results and the corresponding ones. It is observed that the non-dimensional "critical buckling load" β decreases with decreasing the side length and increasing the scale parameter $\sqrt{\zeta}$.

Table 3 Critical buckling load β and critical buckling load ratio $\beta_{NL\ HSDT}/\beta_{L\ HSDT}$ of nonlocal rectangular SLGSs for various non-dimensional nonlocal parameter $\eta=\sqrt{\zeta/a}$

a/b	h/a	η	$\beta(\beta_{NL\ HSDT}/\beta_{L\ HSDT})$									
			Present CPT		Present FSDT		Present HSDT		Zenkour (2016)		Hosseini-Hashemi *et al.* (2015)	
1	0.1	0.0	19.7392	(1.000)	18.6854	(1.000)	18.6877	(1.000)	18.6854	(1.000)	18.6861	(1.000)
		0.1	16.4852	(0.835)	15.6051	(0.835)	15.6070	(0.835)	15.6051	(0.835)	15.6057	(0.835)
		0.2	11.0302	(0.559)	10.4413	(0.559)	10.4426	(0.559)	10.4413	(0.559)	10.4408	(0.559)
		0.3	7.1093	(0.360)	6.7298	(0.360)	6.7306	(0.360)	6.7298	(0.360)	6.7200	(0.360)
		0.4	4.7470	(0.240)	4.4935	(0.240)	4.4941	(0.240)	4.4935	(0.241)	4.4937	(0.241)
	0.01	0.0	19.7392	(1.000)	19.7281	(1.000)	19.7281	(1.000)	19.7281	(1.000)	19.7281	(1.000)
		0.1	16.4852	(0.835)	16.4759	(0.835)	16.4759	(0.835)	16.4759	(0.835)	16.4916	(0.835)
		0.2	11.0302	(0.559)	11.0239	(0.559)	11.0239	(0.559)	11.0239	(0.558)	11.0136	(0.559)
		0.3	7.1093	(0.360)	7.1053	(0.360)	7.1053	(0.360)	7.1053	(0.360)	7.1030	(0.360)
		0.4	4.7470	(0.240)	4.7443	(0.240)	4.7443	(0.240)	4.7443	(0.241)	4.7506	(0.241)
0.5	0.1	0.0	12.3370	(1.000)	11.9169	(1.000)	11.9177	(1.000)	11.9169	(1.000)	11.9171	(1.000)
		0.1	10.9821	(0.890)	10.6082	(0.890)	10.6089	(0.890)	10.6082	(0.890)	10.6084	(0.890)
		0.2	8.2606	(0.670)	7.9793	(0.670)	7.9798	(0.670)	7.9793	(0.670)	7.9794	(0.670)
		0.3	5.8460	(0.474)	5.6470	(0.474)	5.6473	(0.474)	5.6470	(0.474)	6.7289	(0.576)
		0.4	4.1484	(0.336)	4.0072	(0.336)	4.0074	(0.336)	4.1478	(0.336)	4.0072	(0.336)
	0.01	0.0	12.3370	(1.000)	12.3327	(1.000)	12.3327	(1.000)	12.3327	(1.000)	12.3327	(1.000)
		0.1	10.9821	(0.890)	10.9783	(0.890)	10.9783	(0.890)	10.9782	(0.890)	10.9782	(0.890)
		0.2	8.2606	(0.670)	8.2577	(0.670)	8.2577	(0.670)	8.2577	(0.670)	8.2577	(0.670)
		0.3	5.8460	(0.474)	5.8439	(0.474)	5.8439	(0.474)	5.8439	(0.474)	7.1052	(0.576)
		0.4	4.1484	(0.336)	4.1469	(0.336)	4.1469	(0.336)	4.1478	(0.336)	4.1478	(0.336)

Table 3 presents a comparison of the non-dimensional "critical buckling load" β and "critical buckling load ratio" β_{NL}/β_L determined by the present solution (α =1), the solution of Hosseini-Hashemi *et al*. (2015) and the solution of Zenkour (2016) for a rectangular SLGS. The effects of different values of non-dimensional scale parameter (η), geometric ratios (a/b and h/a) on the non-dimensional "buckling loads" and "buckling load ratios" are studied. The computed results are the same as those predicted in Hosseini-Hashemi *et al.* (2015).

In the following, the results are given here (except otherwise stated) for $k_w=10$ nN, $k_p=5$ nN, $\zeta=0.1$ nm2, $\eta=0.1$and $\overline{C}_t=0.1$nN. The appropriate values of the other quantities are fixed as $h=0.34$ nm and $b=10$ nm . Also, the "complex angular frequency" ω is fixed as $\omega=0.5+0.1\,i$. The values of "Young's modulus" $E=1$ GPa and "Poisson's ratio" $\nu=0.3$ are utilized to calculate the numerical "buckling loads".

Table 4 provides the values of β and β_{NL}/β_L of rectangular SLGSs embedded in viscoelastic medium for different values of non-dimensional scale parameter η. Various values of the visco-elastic medium k_w, k_p and $\overline{C}_t$ are also considered in this example. The "critical buckling loads" of the SLGS are very influenced by the inclusion of the "viscoelastic medium". It can be confirmed that there is an excellent agreement with the results given by the FSDT of Zenkour (2016). The "critical buckling loads" are decreasing with the decrease of the coefficients k_w, k_p and $\overline{C}_t$. Also, the "buckling loads" are increased with decreasing the non-dimensional scale parameter. In fact, the important critical buckling load appears for higher values of η and without the inclusion of the "viscoelastic medium".

Fig. 2 presents the variation of the "critical buckling load ratio" $\beta_{NL}^{HSDT}/\beta_{NL}^{CPT}$ versus the geometric ratio a/h of the square SLGS for different values of scale parameters η. It should be noted that β_{NL}^{HSDT} is the "buckling load" obtained by employing the present theory (the four-unknown integral model) and β_{NL}^{CPT} is the "buckling load" obtained by employing the classical plate theory (CPT). It is seen that the buckling loads computed via the CPT are greater than those calculated via the HSDT. This is charged to the shear deformation effect which is neglected by the CPT. In addition, it is observed that the nonlocal parameter

Table 4 Dimensionless critical buckling load β and critical buckling load ratio β_{NL}/β_L of nonlocal rectangular SLGSs for various non-dimensional nonlocal parameter η

$\overline{C}_t$	k_w	k_p	β_{NL}/β_L									
			$\eta=0.0$		$\eta=0.1$		$\eta=0.2$		$\eta=0.3$		$\eta=0.0$	
			Present	HSDT	Present	HSDT	Present	HSDT	Present	HSDT	Present	HSDT
0	0.0	0.0	12.1395	(1.000)	10.8063	(0.890)	8.1283	(0.670)	5.7524	(0.474)	4.0820	(0.336)
0.1	10.0	0.0	17.0029	(1.000)	15.6697	(0.922)	12.9917	(0.764)	10.6158	(0.624)	8.9454	(0.526)
		2.0	19.0029	(1.000)	17.6697	(0.930)	14.9917	(0.789)	12.6158	(0.664)	10.9454	(0.576)
		5.0	22.0029	(1.000)	20.6697	(0.939)	17.9917	(0.1818)	15.6158	(0.710)	13.9454	(0.634)
		10.0	27.0029	(1.000)	25.6697	(0.951)	22.9917	(0.851)	20.6158	(0.763)	18.9454	(0.702)
0.2	10.0	0.0	21.0557	(1.000)	19.7226	(0.937)	17.0446	(0.809)	14.6687	(0.697)	12.9982	(0.617)
		2.0	23.0557	(1.000)	21.7226	(0.942)	19.0446	(0.826)	16.6687	(0.723)	14.9982	(0.651)
		5.0	26.0557	(1.000)	24.7226	(0.949)	22.0446	(0.846)	19.6687	(0.755)	17.9982	(0.691)
		10.0	31.0557	(1.000)	29.7226	(0.957)	27.0446	(0.871)	24.6687	(0.794)	22.9982	(0.741)
0.5	10.0	0.0	33.2143	(1.000)	31.8811	(0.960)	29.2031	(0.879)	26.8272	(0.808)	25.1568	(0.757)
		2.0	35.2143	(1.000)	33.8811	(0.962)	31.2031	(0.886)	28.8272	(0.819)	27.1568	(0.771)
		5.0	38.2143	(1.000)	36.8811	(0.965)	34.2031	(0.895)	31.8272	(0.833)	30.1568	(0.789)
		10.0	43.2143	(1.000)	41.8811	(0.969)	39.2031	(0.907)	36.8272	(0.852)	35.1568	(0.814)

increases the "buckling load ratio" and this effect is more pronounced in thick SLGS.

Fig. 3 shows the effect of damping coefficients $\overline{C}_t$ on the variation of the "critical buckling load ratio" $\beta_{NL}^{HSDT}/\beta_{NL}^{CPT}$ with the geometric ratio a/h of the square SLGS. It is observed that the influence of damping coefficients is more pronounced in thick SLGS. The "buckling load ratio" increase with increasing the damping coefficient and the geometric ratio a/h.

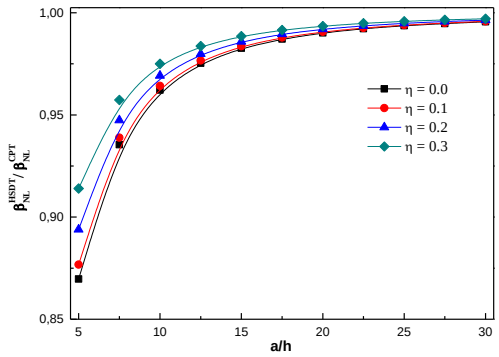

Fig. 2 Critical buckling load ratio $\beta_{NL}^{HSDT}/\beta_{NL}^{CPT}$ versus the side-to thickness ratio a/h of the SLGS for different nonlocal parameters η

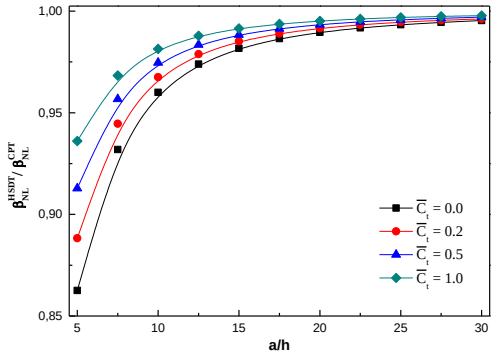

Fig. 3 Critical buckling load ratio $\beta_{NL}^{HSDT}/\beta_{NL}^{CPT}$ versus the side-to thickness ratio a/h of the SLGS for different damping coefficients $\overline{C}_t$

Fig. 4 illustrate the variations of the "critical buckling load ratio" $\beta_{NL}^{HSDT}/\beta_{NL}^{CPT}$ versus the geometric ratio a/h of the square SLGS for different values of Pasternak parameters k_p. Again $\beta_{NL}^{HSDT}/\beta_{NL}^{CPT}$ increase with the increase of the "Pasternak parameter". The effect of k_p is more observed when the nanoplate becomes thick.

Fig. 5 presents the variation of "critical buckling load ratio" $\beta_{NL}^{HSDT}/\beta_{NL}^{CPT}$ versus the geometric ratio a/h of the square SLGS for different mode numbers m and n. It

is clear to note that $\beta_{NL}^{HSDT} / \beta_{NL}^{CPT}$ (m = n = 1) is the greatest one. As the mode numbers increase the ratio $\beta_{NL}^{HSDT} / \beta_{NL}^{CPT}$ is reduced. In additions, as the geometric ratio a/h of the SLGS increases the ratio $\beta_{NL}^{HSDT} / \beta_{NL}^{CPT}$ increases.

The influence of "buckling factor" c on the non-dimensional buckling load is presented in Figs. 6-8. Values of $c<2$ represent compression "buckling loads" while values of $c>2$ represent tension "buckling loads". The results are computed here for $h=0.34$ nm and $n=1$. Two values for the geometric ratio $a/h=5$ and $a/h=20$ are used.

It can be observed that there is a symmetry between the compressive "buckling loads" ($c=0,\ 1$) and the corresponding tensile "buckling loads" ($c=4,\ 3$). Also, the magnitudes of the non-dimensional "buckling loads" of the SLGS with $a/h=5$ are smaller than the "corresponding ones" with $a/h=20$.

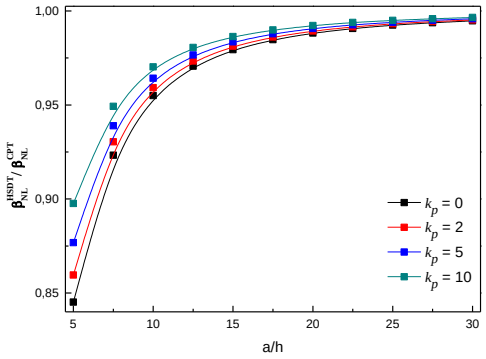

Fig. 4 Critical buckling load ratio $\beta_{NL}^{HSDT} / \beta_{NL}^{CPT}$ versus the side-to thickness ratio a/h of the SLGS for different Pasternak's parameters k_p

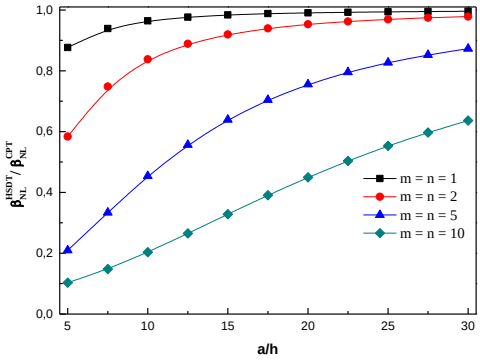

Fig. 5 Critical buckling load ratio $\beta_{NL}^{HSDT} / \beta_{NL}^{CPT}$ versus the side-to thickness ratio a/h of the SLGS for different mode numbers m and n

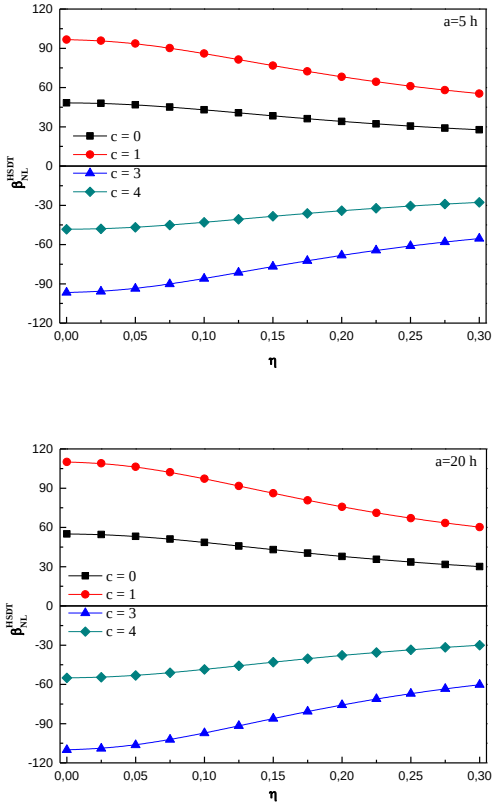

Fig. 6 Nonuniform critical buckling load β_{NL}^{HSDT} vs the nonlocal parameter η of the SLGS for different values of c

Also, as the buckling factor increases the compressive "buckling load" increases while tensile "buckling load" diminishes. The compressive "buckling loads" are diminishing (the tensile "buckling loads" are increasing) with the increase of the scale parameter η, the visco-Pasternak's coefficients $\bar{C}_t$ and k_p as demonstrated in Figs. 6-8.

5. Conclusions

The stability analysis of a single-layered graphene sheet (SLGS) embedded in visco-Pasternak's medium is investigated using nonlocal four-unknown integral model. The effect of transverse shear deformation is also considered without introducing the shear correction factors. The visco-Pasternak's medium is modeled by introducing the damping effect to the classical Winkler-Pasternak elastic foundations. The present model is in good agreement with others models existing in the literature.

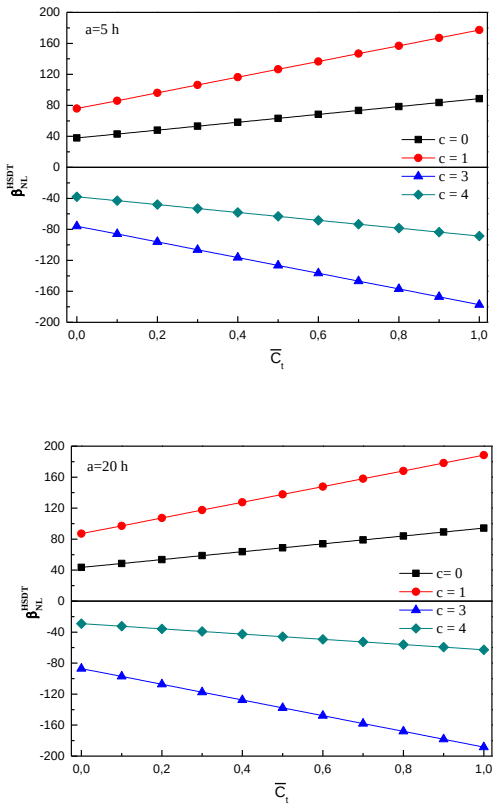

Fig. 7 Nonuniform critical buckling load β_{NL}^{HSDT} vs the damping coefficient $\overline{C}_t$ of the SLGS for different values of c

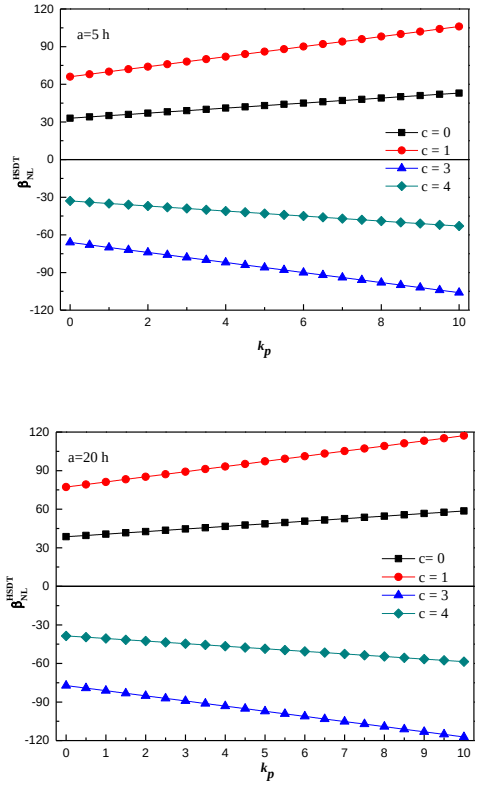

Fig. 8 Non uniform critical buckling load β_{NL}^{HSDT} vs the Pasternak's parameter k_p of the SLGS for different values of c

In can be concluded that the developed model is accurate and efficient to predict the buckling response of the SLGSs under compressive in- plane edge loads and clearly shows the different parameters influencing the critical buckling load. An improvement of the present formulation will be considered in the future work to consider other type of materials (Sharma *et al.* 2009, Sofiyev and Avcar 2010, Avcar 2016, Kolahchi *et al*. 2016, Daouadji 2017, Timesli *et al.* 2017, Kolahchi *et al*. 2017,Ayat *et al.* 2018, Majeed and Sadiq 2018, Behera and Kumari 2018, Hajmohammad *et al.* 2018, Keshtegarand Kolahchi 2018, Hussain and Naeem 2018, Avcar and Mohammed 2018, Belkacem *et al.* 2018, Moghadam *et al.* 2018, Panjehpour *et al*. 2018, Eltaher *et al*. 2018, Shahsavari *et al*. 2019, Nebab *et al*. 2019, Avcar 2019, Mirjavadi *et al.* 2019, Fadoun 2019, Jamali *et al*. 2019, Selmi 2019, Lal *et al.* 2017, Narwariya *et al.* 2018, Pascon 2018, Rezaiee-Pajand *et al.* 2018, Li *et al.* 2018, Othman *et al*. 2019, Akbas 2019a, b, Katariya *et al.* 2019, Yüksela and Akbaş 2018, 2019, Abdou *et al.* 2019, Eltaher *et al.* 2020).

References

Abdou, M.A., Othman, M.I.A., Tantawi, R.S. and Mansour, N.T. (2019), "Exact solutions of generalized thermoelastic medium with double porosity under L–S theory", *Indian J. Phys.*, doi:10.1007/s12648-019-01505-8.

Akbaş, Ş.D. (2016), "Forced vibration analysis of viscoelastic nanobeams embedded in an elastic medium", *Smart Struct. Syst.*, **18**(6), 1125-1143. https://doi.org/10.12989/sss.2016.18.6.1125.

Akbaş, Ş.D. (2018), "Bending of a cracked functionally graded nanobeam", *Adv. Nano Res.*, **6**(3), 219-243. DOI: https://doi.org/10.12989/anr.2018.6.3.219

Akbas, S.D. (2019a). "Hygro-thermal post-buckling analysis of a functionally graded beam", *Coupled Syst. Mech*., **8**(5), 459-471. https://doi.org/10.12989/csm.2019.8.5.459.

Akbas, S.D. (2019b). "Forced vibration analysis of functionally graded sandwich deep beams", *Coupled Syst. Mech*., **8**(3), 259-271. https://doi.org/10.12989/csm.2019.8.3.259.

Akgöz, B. and Civalek, Ö. (2011), "Strain gradient elasticity and modified couple stress models for buckling analysis of axially loaded micro-scaled beams", *Int. J. Eng. Sci*., **49**, 1268-1280.https://doi.org/10.1016/j.ijengsci.2010.12.009

Akgöz, B. and Civalek, Ö. (2012), "Free vibration analysis for single -layered graphene sheets in an elastic matrix via modified couple stress theory", *Mater. Des*., **42**, 164-171.https://doi.org/10.1016/j.matdes.2012.06.002.

Akgöz, B. and Civalek, Ö. (2013a), "A size-dependent shear deformation beam model based on the strain gradient elasticity

theory", *Int. J. Eng. Sci.*, **70**, 1-14. https://doi.org/10.1016/j.ijengsci.2013.04.004.

Akgöz, B. and Civalek, Ö. (2013b), "Buckling analysis of functionally graded microbeams based on the strain gradient theory", *Acta Mech*., **224**, 2185-2201. DOI 10.1007/s00707-013-0883-5.

Akgöz, B. and Civalek, Ö. (2013c), "Free vibration analysis of axially functionally graded tapered Bernoulli – Euler microbeams based on the modified couple stress theory", *Compos. Struct*., **98**, 314-322. https://doi.org/10.1016/j.compstruct.2012.11.020.

Anjomshoa, A., Shahidi, A.R., Hassani B. and Jomehzadeh, E. (2014), "Finite element buckling analysis of multi-layered graphene sheets on elastic substrate based on nonlocal elasticity theory", *Appl. Math. Model*., **38**, 5934-5955.https://doi.org/10.1016/j.apm.2014.03.036.

Ansari, R. and Sahmani, S. (2013), "Prediction of biaxial buckling behavior of single-layered graphene sheets based on nonlocal plate models and molecular dynamics simulations", *Appl. Math. Model*., **37**, 7338-7351. https://doi.org/10.1016/j.apm.2013.03.004.

Avcar, M. (2016), "Effects of material non-homogeneity and two parameter elastic foundation on fundamental frequency parameters of Timoshenko beams", *Acta Physica Polonica A*, **130**(1), 375-378.

Avcar, M. (2019), "Free vibration of imperfect sigmoid and power law functionally graded beams", *Steel Compos. Struct.*, **30**(6), 603-615. https://doi.org/10.12989/scs.2019.30.6.603.

Avcar, M. and Mohammed, W.K.M. (2018), "Free vibration of functionally graded beams resting on Winkler-Pasternak foundation", *Arabian J. Geosci.*, **11**(10), 232.

Ayat, H., Kellouche, Y., Ghrici, M. and Boukhatem, B. (2018), "Compressive strength prediction of limestone filler concrete using artificial neural networks", *Adv. Comput. Design*, **3**(3), 289-302. https://doi.org/10.12989/acd.2018.3.3.289

Barati, M.R. and Shahverdi, H. (2019). "Finite element forced vibration analysis of refined shear deformable nanocompositegraphene platelet-reinforced beams", *J. Brazilian Soc. Mech. Sci. Eng*., **42**(1). doi:10.1007/s40430-019-2118-8.

Basua, S. and Bhattacharyya, P. (2012), "Recent developments on graphene and graphene oxide based solid state gas sensors", *Sens. Actuat. B*, **173**, 1-21. https://doi.org/10.1016/j.snb.2012.07.092

Behera, S. and Kumari, P. (2018), "Free vibration of Levy-type rectangular laminated plates using efficient zig-zag theory", *Adv. Comput. Design*, **3**(3), 213-232. https://doi.org/10.12989/acd.2018.3.3.213

Belkacem, A., Tahar, H.D., Abderrezak, R., Amine, B.M., Mohamed, Z. and Boussad, A. (2018), "Mechanical buckling analysis of hybrid laminated composite plates under different boundary conditions", *Struct. Eng. Mech.*, **66**(6), 761-769. https://doi.org/10.12989/sem.2018.66.6.761.

Belmahi, S., Zidour, M. and Meradjah, M. (2019), "Small-scale effect on the forced vibration of a nano beam embedded an elastic medium using nonlocal elasticity theory", *Adv. Aircraft Spacecraft Sci.*, **6**(1), 1-18.

Belmahi, S., Zidour, M., Meradjah, M., Bensattalah, T. and Dihaj, A. (2018), "Analysis of boundary conditions effects on vibration of nanobeam in a polymeric matrix", *Struct. Eng. Mech.*, **67**(5), 517-525. https://doi.org/10.12989/sem.2018.67.5.517.

Bensattalah, T., Bouakkaz, K., Zidour, M. and Daouadji, T.H. (2018a), "Critical buckling loads of carbon nanotube embedded in Kerr's medium", *Adv. Nano Res.*, **6**(4), 339-356. https://doi.org/10.12989/anr.2018.6.4.339.

Bensattalah, T., Zidour, M. and Hassaine Daouadji, T. (2018b), "Analytical analysis for the forced vibration of CNT surrounding elastic medium including thermal effect using nonlocal Euler-Bernoulli theory", *Adv. Mater. Res.*, **7**(3), 163-174.

Bensattalah, T., Zidour, M., HassaineDaouadji, T. and Bouakaz, K. (2019), "Theoretical analysis of chirality and scale effects on critical buckling load of zigzag triple walled carbon nanotubes under axial compression embedded in polymeric matrix", *Struct. Eng. Mech.*, **70**(3), 269-277. https://doi.org/10.12989/sem.2019.70.3.269.

Daouadji, T.H. (2017), "Analytical and numerical modeling of interfacial stresses in beams bonded with a thin plate", *Adv. Comput. Design*, ,**2**(1), 57-69. DOI: https://doi.org/10.12989/acd.2017.2.1.057.

Dihaj, A., Zidour, M., Meradjah, M., Rakrak, K., Heireche, H. and Chemi, A. (2018), "Free vibration analysis of chiral double-walled carbon nanotube embedded in an elastic medium using non-local elasticity theory and Euler Bernoulli beam model", *Struct. Eng. Mech.*, **65**(3), 335-342. https://doi.org/10.12989/sem.2018.65.3.269.

Ebrahimi, F. and Barati, M.R. (2017), "Scale-dependent effects on wave propagation in magnetically affected single/double-layered compositionally graded nanosize beams", *Waves Random Complex Media.*, **28**(2), 326 342. doi:10.1080/17455030.2017.1346331.

Ebrahimi, F. and Barati, M.R. (2017a), "Buckling analysis of nonlocal strain gradient axially functionally graded nanobeams resting on variable elastic medium", *Proceedings of the Institution of Mechanical Engineers, Part C: Journal of Mechanical Engineering Science*., **232**(11), 2067-2078. doi:10.1177/0954406217713518.

Eltaher, M.A., El-Borgi, S. and Reddy, J.N. (2016), "Nonlinear analysis of size-dependent and material-dependent nonlocal CNTs", *Compos. Struct*., **153**, 902-913. doi:10.1016/j.compstruct.2016.07.013.

Eltaher, M.A., Mohamed, S.A. and Melaibari, A. (2020), "Static stability of a unified composite beams under varying axial loads", *Thin-Wall. Struct*., **147**, 106488. doi:10.1016/j.tws.2019.106488.

Eltaher, M.A., Almalki, T.A. and Ahmed, K.I.E. (2019), "Characterization and behaviors of single walled carbon nanotube by equivalent-continuum mechanics approach", *Adv. Nano Res.*, **7**(1), 39-49. https://doi.org/10.12989/anr.2019.7.1.039.

Eltaher, M.A., Emam, S.A. and Mahmoud, F.F. (2013), "Static and stability analysis of nonlocal functionally graded nanobeams", *Compos. Struct.*, **96**, 82-88.

Eltaher, M.A., Fouda, N., El-Midany, T. and Sadoun, A.M. (2018), "Modified porosity model in analysis of functionally graded porous nanobeams", *J. Brazilian Soc. Mech. Sci. Eng.*, **40**,141. https://doi.org/10.1007/s40430-018-1065-0.

Eltaher, M.A., Agwa, M. and Kabeel, A. (2018), "Vibration Analysis of Material Size-Dependent CNTs Using Energy Equivalent Model", *J. Appl. Comput. Mech*., **4**(2), 75-86. doi:10.22055/JACM.2017.22579.1136.

Eringen, A.C. (1972), "Nonlocal polar elastic continua", *Int. J. Eng. Sci.*, **10**, 1-16. https://doi.org/10.1016/0020-7225(72)90070-5.

Eringen, A.C. (1983), "On differential equations of nonlocal elasticity, solutions of screw dislocation, surface waves", *J. Appl. Phys.*, **54**, 4703-4710. DOI:10.1063/1.332803.

Eringen, A.C. (2006), "Nonlocal continuum mechanics based on distributions", *Int. J. Eng. Sci*., **44**, 141-147.https://doi.org/10.1016/j.ijengsci.2005.11.002.

Eringen, A.C. and Edelen, D.G.B. (1972), "On nonlocal elasticity", *Int. J. Eng. Sci*., **10**, 233-248. https://doi.org/10.1016/0020-7225(72)90039-0.

Fadoun, O.O. (2019), "Analysis of axisymmetric fractional

vibration of an isotropic thin disc in finite deformation", *Comput. Concrete*, **23**(5), 303-309. DOI: https://doi.org/10.12989/cac.2019.23.5.303

Farajpour, A., Dehghany, M. and Shahidi, A.R. (2013b), "Surface and nonlocal effects on the axisymmetric buckling of circular graphene sheets in thermal environment", *Compos B*, **50**, 333-343. https://doi.org/10.1016/j.compositesb.2013.02.026.

Farajpour, A., Solghar, A.A. and Shahidi, A. (2013a), "Postbuckling analysis of multi-layered graphene sheets under non-uniform biaxial compression", *Phys. E*, **47**, 197-206. https://doi.org/10.1016/j.physe.2012.10.028.

Forsat, M., Badnava, S., Mirjavadi, S.S., Barati, M.R. and Hamouda, A.M.S. (2020), "Small scale effects on transient vibrations of porous FG cylindrical nanoshells based on nonlocal strain gradient theory", *The European Physical J. Plus*., **135**(1). doi:10.1140/epjp/s13360-019-00042-x..

GhorbanpourArani, A., Amir, S., Dashti, P. and Yousefi, M. (2014), "Flow-induced vibration of double bonded visco-CNTs under magnetic fields considering surface effect", *Comput. Mater. Sci.*, **86**, 144-154. https://doi.org/10.1016/j.commatsci.2014.01.047.

Golmakani, M.E. and Rezatalab, J. (2015), "Nonuniform biaxial buckling of orthotropic nanoplates embedded in an elastic medium based on nonlocal Mindlin plate theory", *Compos. Struct*., **119**, 238-250. https://doi.org/10.1016/j.compstruct.2014.08.037.

Hajmohammad, M.H., Zarei, M.S., Farrokhian, A. and Kolahchi, R. (2018), "A layerwise theory for buckling analysis of truncated conical shells reinforced by CNTs and carbon fibers integrated with piezoelectric layers in hygrothermal environment", *Adv. Nano Res*., **6**(4), 299-321. https://doi.org/10.12989/anr.2018.6.4.299.

Hamidi, A., Zidour, M., Bouakkaz, K. and Bensattalah, T. (2018), "Thermal and small-scale effects on vibration of embedded armchair single-walled carbon nanotubes", *J. Nano Res.*, **51**, 24-38.

Hussain, M. and Naeem, M.N. (2019), "Rotating response on the vibrations of functionally graded zigzag and chiral single walled carbon nanotubes", *Appl. Math. Model.*, **75**, 506-520. https://doi.org/10.1016/j.apm.2019.05.039.

Jamali, M., Shojaee, T., Mohammadi, B. and Kolahchi, R. (2019), "Cut out effect on nonlinear post-buckling behavior of FG-CNTRC micro plate subjected to magnetic field via FSDT", *Adv. Nano Res*., **7**(6), 405-417. https://doi.org/10.12989/anr.2019.7.6.405.

Karami, B. and Janghorban, M. (2019), "A new size-dependent shear deformation theory for free vibration analysis of functionally graded/anisotropic nanobeams", *Thin-Wall. Struct.*, **143**, 106-227. https://doi.org/10.1016/j.tws.2019.106227.

Karami, B. and Karami, S. (2019), "Buckling analysis of nanoplate-type temperature-dependent heterogeneous materials", *Adv. Nano Res.*, **7**(1), 51-61. DOI: https://doi.org/10.12989/anr.2019.7.1.051.

Karlicic, D., Cajic, M., Kozic, P. and Pavlovic, I. (2015), "Temperature effect s on the vibration and stability behavior of multi-layered graphene sheets embedded in an elastic medium", *Compos. Struct*., **131**, 672-681. https://doi.org/10.1016/j.compstruct.2015.05.058.

Katariya, P.V., Hirwani, C.K. and Panda, S.K. (2019), "Geometrically nonlinear deflection and stress analysis of skew sandwich shell panel using higher-order theory", *Eng. with Comput.*, **35**(2), 467-485. https://doi.org/10.1007/s00366-018-0609-3.

Ke, L.L., Wang, Y.S., Yang, J. and Kitipornchai, S. (2012), "Free vibration of size-dependent Mindlinmicroplates based on the modified couple stress theory", *J. Sound Vib*., **331**, 94-106. https://doi.org/10.1016/j.jsv.2011.08.020.

Keshtegar, B. and Kolahchi, R. (2018), "Reliability analysis-based conjugate map of beams reinforced by ZnO nanoparticles using sinusoidal shear deformation theory", *Steel Compos. Struct.*, **28**(2), 195-207. https://doi.org/10.12989/scs.2018.28.2.195.

Kolahchi, R., Safari, M. and Esmailpour, M. (2016), "Dynamic stability analysis of temperature-dependent functionally graded CNT-reinforced visco-plates resting on orthotropic elastomeric medium", *Compos. Struct*., **150**, 255-265. doi:10.1016/j.compstruct.2016.05.023.

Kolahchi, R., Zarei, M.S., Hajmohammad, M.H. and Nouri, A. (2017), "Wave propagation of embedded viscoelastic FG-CNT-reinforced sandwich plates integrated with sensor and actuator based on refined zigzag theory", *Int. J. Mech. Sci*., **130**, 534-545. doi:10.1016/j.ijmecsci.2017.06.039.

Lal, A., Jagtap, K.R. and Singh, B.N. (2017), "Thermo-mechanically induced finite element based nonlinear static response of elastically supported functionally graded plate with random system properties", *Adv. Comput. Design*, **2**(3), 165-194. https://doi.org/10.12989/acd.2017.2.3.165.

Lam, D.C.C., Yang, F., Chong, A.C.M., Wang, J. and Tong, P. (2003), "Experiments and theory in strain gradient elasticity", *J. Mech. Phys. Solid.*, **51**, 1477-1508. https://doi.org/10.1016/S0022-5096(03)00053-X.

Li, F., Li, J., Feng, Y., Yang, L. and Du, Z. (2011), "Electrochemical behavior of graphene doped carbon paste electrode and its application for sensitive determination of ascorbic acid", *Sens. Actuat. B*, **157**, 110-114. DOI: 10.1016/j.snb.2011.03.033.

Li, D.H., Guo, Q.R., Xu, D. and Yang, X. (2017), "Three-dimensional micromechanical analysis models of fiber reinforced composite plates with damage", *Comput. Struct*., **191**, 100-114. https://doi.org/10.1016/j.compstruc.2017.06.005.

Lim, C.W., Li, C. and Yu, J.L. (2010), "Dynamic behaviour of axially moving nanobeams based on nonlocal elasticity approach", *Acta Mech. Sinica*, **26**, 755-765. doi:10.1007/s10409-010-0374-z.

Liu, J., Chen, L., Xie, F., Fan, X. and Li, C. (2016), "On bending, buckling and vibration of graphenenanosheets based on the nonlocal theory", *Smart Struct. Syst*., **17**(2), 257-274. https://doi.org/10.12989/eas.2016.17.2.257.

Majeed, W.I. and Sadiq, I.A. (2018), "Buckling and pre stressed vibration analysis of laminated plates using new shear deformation", *IOP Conf. Ser.: Mater. Sci. Eng*., **454**, 012006. https://doi.org/10.1088/1757-899X/454/1/012006.

Mirjavadi, S.S., Forsat, M. and Badnava, S. (2019), "Nonlinear modeling and dynamic analysis of bioengineering hyper-elastic tubes based on different material models", *Biomech Model Mechanobiol,* (In press). doi:10.1007/s10237-019-01265-8

Moghadam, A., Estekanchi, H.E. and Yekrangnia, M. (2018), "Evaluation of PR steel frame connection with torsional plate and its optimal placement", *Sci. Iran*., **25**(3), 1025-1038. DOI: 10.24200/SCI.2017.4196

Mohamed, N., Eltaher, M.A., Mohamed, S.A. and Seddek, L.F. (2019), "Energy equivalent model in analysis of postbuckling of imperfect carbon nanotubes resting on nonlinear elastic foundation", *Struct. Eng. Mech.*, **70**(6), 737-450. https://doi.org/10.12989/sem.2019.70.6.737.

Mohammadi, M., Farajpour, A., Moradi, A. and Ghayour, M. (2014), "Shear buckling of orthotropic rectangular graphene sheet embedded in an elastic medium in thermal environment", *Compos. B*, **56**, 629-637. https://doi.org/10.1016/j.compositesb.2013.08.060.

Narwariya, M., Choudhury, A. and Sharma, A.K. (2018), "Harmonic analysis of moderately thick symmetric cross-ply laminated composite plate using FEM", *Adv. Comput. Design*, **3**(2), 113-132. https://doi.org/10.12989/acd.2018.3.2.113.

Nebab, M., AitAtmane, H., Bennai, R. and Tahar, B. (2019), "Effect of nonlinear elastic foundations on dynamic behavior of

FG plates using four-unknown plate theory", *Earthq. Struct.*, **17**(5), 447-462. https://doi.org/10.12989/eas.2019.17.5.447.

Novoselov, K.S., Geim, A.K., Morozov, S.V., Jiang, D., Zhang, Y., Dubonos, S.V., Grigorieva, I.V. and Firsov, A.A. (2004), "Electric field effect in atomically thin carbon films", *Science*, **306**, 666-669.DOI: 10.1126/science.1102896

Othman, M.I.A., Abouelregal, A.E. and Said, S.M. (2019), "The effect of variable thermal conductivity on an infinite fiber-reinforced thick plate under initial stress", *J. Mech. Mater. Struct*., **14**(2), 277-293. doi:10.2140/jomms.2019.14.277.

Panjehpour, M., Woo, E., Loh, K. and Deepak, TJ. (2018), "Structural insulated panels: State-of-the-art", *Trends in civil Engineering and its architecture*, **3**(1) 336-340. 10.32474/TCEIA.2018.03.000151

Pantelic, R.S., Meyer, J.C., Kaiser, U. and Stahlberg, H. (2012), "The application of graphene as a sample support in transmission electron microscopy", *Solid State Commun*., **152**, 1375-1382. https://doi.org/10.1016/j.ssc.2012.04.038

Pascon, J.P. (2018), "Large deformation analysis of functionally graded visco-hyperelastic materials", *Comput. Struct.*, **206**, 90-108. https://doi.org/10.1016/j.compstruc.2018.06.001.

Pradhan, S.C. and Murmu, T. (2009), "Small scale effect on the buckling of single -layered graphene sheets under biaxial compression via nonlocal continuum mechanics", *Comput. Mater. Sci*., **47**, 268-274. https://doi.org/10.1016/j.commatsci.2009.08.001

Pradhan, S.C. and Murmu, T. (2010), "Small scale effect on the buckling analysis of single-layered graphene sheet embedded in an elastic medium based on nonlocal plate theory", *Phys. E*, **42**, 1293-1301. https://doi.org/10.1016/j.physe.2009.10.053.

Radic, N., Jeremic, D., Trifkovic, S. and Milutinovic, M. (2014), "Buckling analysis of double –orthotropic nanoplates embedded in Pasternak elastic medium using nonlocal elasticity theory", *Compos. B*, **61**, 162-171. https://doi.org/10.1016/j.compositesb.2014.01.042.

Reddy, J.N. (1984), "A simple higher-order theory for laminated composite plates", *J. Appl. Mech.*, **51**(4), 745-752. https://doi.org/10.1115/1.3167719.

Reddy, J.N. (2011), "Microstructure-dependent couple stress theories of functionally graded beams", *J. Mech. Phys. Solid*., **59**, 2382-2399. https://doi.org/10.1016/j.jmps.2011.06.008.

Rezaiee-Pajand, M., Masoodi, A.R. and Mokhtari, M. (2018), "Static analysis of functionally graded non-prismatic sandwich beams", *Adv. Comput. Design*, **3**(2), 165-190. https://doi.org/10.12989/acd.2018.3.2.165.

Safaei, B., Khoda, F.H. and Fattahi, A.M. (2019), "Non-classical plate model for single-layered graphene sheet for axial buckling", *Adv Nano Res*., **7**(4), 265-275. https://doi.org/10.12989/anr.2019.7.4.265.

Sakhaee-Pour, A., Ahmadian, M.T. and Vafai, A. (2008), "Applications of single-layered graphene sheets as mass sensors and atomistic dust detectors", *Solid State Commun*., **145**, 168-172. https://doi.org/10.1016/j.ssc.2007.10.032.

Samaei, A.T., Abbasion, S. and Mirsayar, M.M. (2011), "Buckling analysis of a single-layer graphene sheet embedded in an elastic medium based on nonlocal Mindlin plate theory", *Mech. Res. Commun*., **38**, 481-485. https://doi.org/10.1016/j.mechrescom.2011.06.003.

Selmi, A. (2019), "Effectiveness of SWNT in reducing the crack effect on the dynamic behavior of aluminium alloy", *Adv. Nano Res.*, **7**(5), 365-377. https://doi.org/10.12989/anr.2019.7.5.365.

Shahsavari, D., Karami, B. and Janghorban, M. (2019), "On buckling analysis of laminated composite plates using a nonlocal refined four-variable model", *Steel Compos. Struct.*, **32**(2), 173-187. https://doi.org/10.12989/scs.2019.32.2.173.

Sharma, J.N., Chand, R. and Othman, M.I.A. (2009), "On the propagation of Lamb waves in viscothermoelastic plates under fluid loadings", *Int. J. Eng. Sci*., **47**(3), 391–404. doi:10.1016/j.ijengsci.2008.10.008.

Sofiyev, A.H. and Avcar, M. (2010), "The stability of cylindrical shells containing an FGM layer subjected to axial load on the Pasternak foundation", *Engineering*, **2**(4), 228.

Soleimani, A., Dastani, K., Hadi, A. and Naei, M.H. (2019), "Effect of out-of-plane defects on the postbuckling behavior of graphene sheets based on nonlocal elasticity theory", *Steel Compos. Struct.*, **30**(6), 517-534. https://doi.org/10.12989/scs.2019.30.6.517.

Timesli, A., Braikat, B., Jamal, M. and Damil, N. (2017), "Prediction of the critical buckling load of multi-walled carbon nanotubes under axial compression", *Comptes Rendus Mcanique*, **345**, 158-168. https://doi.org/10.1016/j.crme.2016.12.002.

Wang, J., Li, Z., Fan, G., Pan, H., Chen, Z. and Zhang, D. (2012), "Reinforcement with graphenenano- sheets in aluminum matrix composites", *Scripta Mater*., **66**, 594-597.https://doi.org/10.1016/j.scriptamat.2012.01.012.

Xu, Y.M., Shen, H.S. and Zhang, C.L. (2013), "Nonlocal plate model for nonlinear bending of bilayer graphene sheets subjected to transverse loads in thermal environments", *Compos. Struct*., **98**, 294-302. https://doi.org/10.1016/j.compstruct.2012.10.041.

Yang, F., Chong, A.C.M., Lam, D.C.C. and Tong, P. (2002), "Couple stress based strain gradient theory for elasticity", *Int. J. Solid. Struct.*, **39**, 2731-2743. https://doi.org/10.1016/S0020-7683(02)00152-X.

Yüksela, Y.Z., and Akbaş, S.D. (2019), "Buckling analysis of a fiber reinforced laminated composite plate with porosity", *J. Comput. Appl. Mechanics*., **50**(2), 375-380. DOI: 10.22059/jcamech.2019.291967.448.

Yüksela, Y.Z., and Akbaş, S.D. (2018), "Free vibration analysis of a cross-ply laminated plate in thermal environment", *Int. J. Eng. Appl. Sci. (IJEAS)*., **10**(3), 176-189. http://dx.doi.org/10.24107/ijeas.456755.

Zenkour, A.M. (2016), "Buckling of a single-layered graphene sheet embedded in visco-Pasternak's medium via nonlocal first-order theory", *Adv. Nano Res.*, **4**(4), 309-326. https://doi.org/10.12989/anr.2016.4.4.309.

Zhang, Y., Zhang, L.W., Liew, K.M. and Yu, J.L. (2016) "Buckling analysis of graphene sheets embedded in an elastic medium based on the kp-Ritz method and non-local elasticity theory", *Eng. Anal. Bound. Elem*., **70**, 31-39.https://doi.org/10.1016/j.enganabound.2016.05.009.

CC